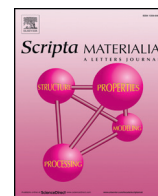




Contents lists available at ScienceDirect

Scripta Materialia

journal homepage: [www.elsevier.com/locate/scriptamat](http://www.elsevier.com/locate/scriptamat)

Viewpoint article

## Additive manufacturing of near-net-shape bonded magnets: Prospects and challenges

Ling Li<sup>a</sup>, Brian Post<sup>b</sup>, Vlastimil Kunc<sup>b</sup>, Amy M. Elliott<sup>b</sup>, M. Parans Paranthaman<sup>a,\*</sup><sup>a</sup> Chemical Sciences Division, Oak Ridge National Laboratory, Oak Ridge, TN 37831, USA<sup>b</sup> Manufacturing Demonstration Facility, Oak Ridge National Laboratory, TN 37932, USA

## ARTICLE INFO

## Article history:

Received 21 September 2016

Received in revised form 27 December 2016

Accepted 28 December 2016

Available online xxxx

## Keywords:

3D printing

NdFeB

Bonded magnets

Binder jetting

Big Area Additive Manufacturing

## ABSTRACT

Additive manufacturing (AM) or 3D printing is well known for producing arbitrary shaped parts without any tooling required, offering a promising alternative to the conventional injection molding method to fabricate near-net-shaped magnets. In this viewpoint, we compare two 3D printing technologies, namely binder jetting and material extrusion, to determine their applicability in the fabrication of Nd-Fe-B bonded magnets. Prospects and challenges of these state-of-the-art technologies for large-scale industrial applications will be discussed.

Published by Elsevier Ltd. on behalf of Acta Materialia Inc.

## 1. Introduction

Permanent magnets (PM) refer to materials with a broad hysteresis loop; they are widely used in areas in which an energy conversion, usually from electrical to mechanical energy, is required, such as in motors and hard disk drives [1]. Another fact about permanent magnet is that they consist of a large amount of rare-earth (RE) elements such as Nd, Dy and Tb, majority of which are mined and separated in China, and US is experiencing a “rare earth crisis”. As the strongest PM, Nd<sub>2</sub>Fe<sub>14</sub>B based magnets occupy 2/3 of the PM market even though they cost 25 times as that of the hard ferrites (BaFe<sub>12</sub>O<sub>19</sub>). In response to address this RE criticality, considerable research efforts have been made to develop heavy RE free and/or reduced RE permanent magnets [2–4]. However, this approach involves screening tremendous number of compositions resulting in slow progress.

One of the alternative strategies to diversify the critical materials supply and lower the PM cost is to reduce the material waste associated with the manufacturing (e.g., cutting, machining, etc.) which cannot be readily re-used. The state-of-the-art technology additive manufacturing (AM) is well-suited to fabricate magnets which frequently involve the expensive and critical RE elements. As opposed to conventional subtractive manufacturing, AM produces complex shaped objects through joining materials in a layer-upon-layer fashion based on a computer-aided-design (CAD). Owing to this unique fabrication method, AM exhibits

significant advantages such as reduced materials waste and energy consumption, no machining/tooling required and low labor cost, etc. To date, the majority of the additive efforts have been focused on structural materials such as fiber-reinforced composites [5] and alloys [6–8], etc., whereas AM of functional materials such as magnets is still in its infancy. Laser metal printing has been utilized to rapidly synthesize Fe-Co magnets with varying compositions, enabling fast assessment of magnetic properties of this binary system [9]. Nevertheless, metal printing of NdFeB magnets is more challenging owing to the high melting temperature, different evaporation rates of each element and the complexity in the ternary phase diagram. Very recently, extrusion printing of NdFeB bonded magnets have been explored [10,11]. Huber *et al.*, reported the fabrication of Nylon bonded NdFeB magnet with a commercial 3D printer [10]. The magnetic powder loading fraction is 54 vol.%, and the density of the printed magnet is 3.6 g/cm<sup>3</sup>, which is lower than that of the injection molded samples, indicating a higher level of porosity in the 3D printed samples [10]. Compton *et al.* fabricated NdFeB bonded magnets with a direct-write 3D-printer via an epoxy-based thermoset ink composed of 40 vol.% anisotropic MQA powder and 60 vol.% epoxy [11]. ASTM F42 committee classified AM into seven categories including directed energy deposition, powder bed fusion, binder jetting, and material extrusion, etc. [12]. In this viewpoint, we compare the feasibility of two of these technologies, namely binder jetting and material extrusion, for fabricating near-net-shape NdFeB bonded magnets. In particular, we demonstrate that the material extrusion method using the Big Area Additive Manufacturing (BAAM) system is superior in fabricating bonded magnets with magnetic and mechanical

\* Corresponding author.

E-mail address: [paranthamanm@ornl.gov](mailto:paranthamanm@ornl.gov) (M.P. Paranthaman).

properties comparable to those produced by conventional injection molding method. The prospects and challenges of permanent magnets AM being adopted for industrial production will be evaluated.

## 2. Bonded magnets

Bonded magnets are fabricated by mixing the magnet powder with a polymer binder (e.g. nylon, epoxy, etc.), then molded into desired shapes via, conventionally, injection molding, compression molding, extrusion etc. [13]. The volume fraction of magnetic powder in injection and compression molding is typically 65% and 80%, respectively [13]. Compared to sintered magnets, bonded magnets have enhanced freedom in terms of geometry, and are more cost effective but at the expense of reduced energy product  $BH_{max}$  due to the incorporation of the non-ferromagnetic polymer binder [14]. In terms of mechanical properties, bonded magnets present a better ductility while lower tensile strength. The shape flexibility of bonded magnets enables innovative designs for motor magnets, which can potentially increase the torque output.

## 3. Binder jetting with ExOne X1-Lab

Binder jetting involves a liquid binder which is selectively deposited into a powder bed to bind materials to form complex shaped parts. It is suited to print magnets as it does not employ heat during the build process. Upon printing completion, the printed magnet is then placed in an oven at 100–150 °C to cure the thermoset binder. A detailed description of the set up and working principle of the ExOne X1-Lab printer is available in Ref. [15,16]. This AM technique has been shown to fabricate various metals [17], ceramics [18,19], and functional solid oxide fuel cells [16], etc. In this work, we printed NdFeB bonded magnets using two kinds of magnet powders - isotropic MQP-B-20173-070 (Magnequench) and anisotropic magfine powder MF18P (Aichi Steel), respectively. Fig. 1(a) shows some images of the printed magnets with a horseshoe, square, and ring shape. Fig. 1(b) presents the demagnetization curves of the parts printed with the isotropic powder MQP-B. The printing process did not degrade the intrinsic coercivity  $H_{ci}$  at all.

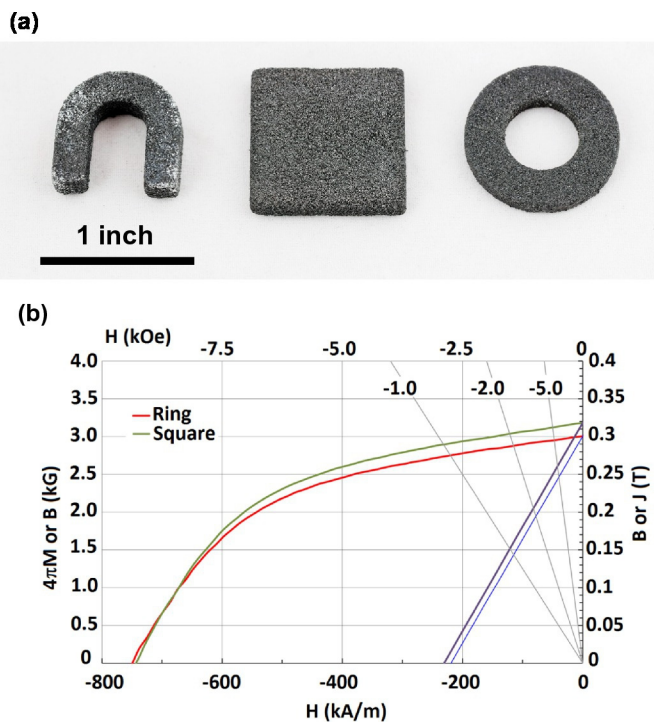


Fig. 1. (a) Images of the binder jet printed NdFeB magnets with different shapes; (b) magnetic properties of the binder jet printed NdFeB magnets using MQP-B powder. (reprinted with permission from Ref. [15]).

Density of the magnetic phase is essential to ensure magnet functionality as it determines how much magnetic flux the magnet can generate in a given space. Here, the measured density of the printed MQP-B magnet is 3.3 g/cm<sup>3</sup>, which is nearly 43% dense compared to the theoretical magnet crystal density. The low density is related to the low volume fraction of the magnet powder as well as the inter layer and/or inter particle porosity. In fact, the commercially available thermoset binder from the ExOne company needs some improvement in terms of binding ability, and efforts are being made to apply stronger polymer binders to this 3D printing system.

Densification is a long-term challenge for binder jetting. Bimodal powders with varying particle sizes can be introduced during printing to improve the packing density. Furthermore, post-processing steps such as infiltration with nano-particles are frequently carried out to fill the voids and enhance mechanical strength [20]. For example, bronze was diffused into binder jetted stainless steel at 1050 °C to achieve full density. In the research community of permanent magnet, grain boundary diffusion process (GBDP) using low-melting point alloy (e.g., Nd-Cu) is a well-known method to effectively enhance coercivity through modifying the intergranular phase between the magnetic Nd<sub>2</sub>Fe<sub>14</sub>B grains [21]. Thus, it is of interest to apply this technique, optimally, with the application of expansion constraint to minimize the loss of remanence [22], to the binder jetted magnets to achieve densification, and meanwhile, improve coercivity.

With the downsizing of electronics, bonded magnets with higher energy product  $BH_{max}$  are strongly desirable. This can be achieved through magnetically aligning anisotropic powder during the manufacturing process to increase the remanence  $B_r$  as well as the density of the final part [23]. Dy free magfine powder MF18P with  $H_{ci} = 14.2$  kOe was used to explore the feasibility of *in-situ* alignment during the printing process. However, *in-situ* alignment remains a major challenge for binder jetting as the distance between the print head and the powder bed is very small; once the powder is aligned, it interferes with the print head directly, which could damage the print head. Alternatively, in this study, alignment with a sintered NdFeB magnet which was placed at the bottom of the printed part was carried out during the post-curing stage in an oven at 100 °C. The magnetic field generated by the sintered magnet for the alignment is approximately 1 T. The density and magnetic characteristics of the printed magnets without and with alignment are summarized in Table 1. It can be seen that the alignment enhanced the density and remanence  $B_r$ , resulting in a  $BH_{max}$  enhancement from 2.4 to 3.8 MGOe. Further efforts are under way to realize *in-situ* alignment.

## 4. Material extrusion with the Big Area Additive Manufacturing (BAAM) system

BAAM is a system developed by a team of researchers from ORNL's Manufacturing Demonstration Facility and Cincinnati Inc. to fabricate large-scale parts via a material extrusion method [24]. BAAM deposits molten thermoplastics in a layer-upon-layer fashion – the materials are extruded from the nozzle and solidify rapidly [25]. Fig. 2 shows a schematic of the BAAM process for fabricating NdFeB bonded magnets. Magnequench isotropic MQP B + powder (65 vol.%) was mixed uniformly with Nylon-12 (35 vol.%), and extruded first to obtain composite pellets, which were then used as feedstock materials in BAAM. Note that BAAM does not require pre-fabrication of filament. The temperature at the orifice exit of the extruder was approximately 270 °C, and the printed magnet was then polished and coated with a polyurethane polymer by TruDesign LLC.

Table 1  
Characteristics of binder jetted NdFeB bonded magnets with anisotropic MF18P powder.

Sample	Density (g/cm <sup>3</sup> )	$H_{ci}$ (kOe)	$B_r$ (kG)	$BH_{max}$ (MGOe)
Without alignment	3.54	14.2	3.3	2.4
Aligned during curing	3.86	14.2	4.2	3.8

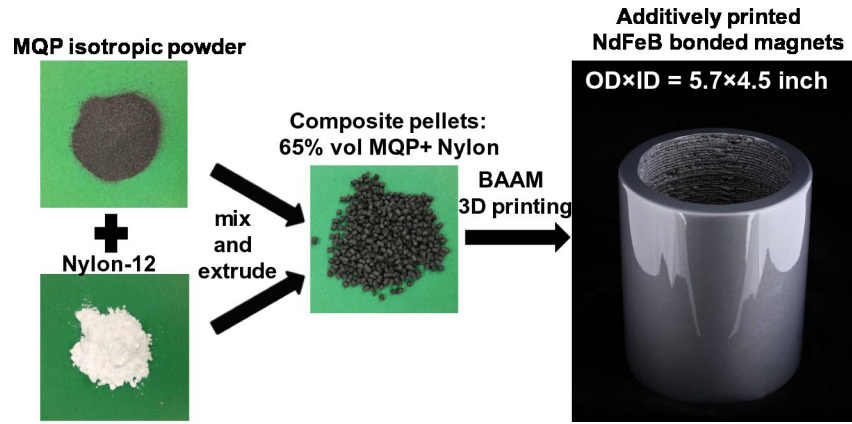


**Fig. 2.** Schematic of fabricating NdFeB bonded magnet in which the magnet powder is mixed with nylon-12, and extruded to obtain composite pellets, which are used as feedstock materials for BAAM printing. The picture on the right shows a hollow cylinder magnet with an OD  $\times$  ID of  $\sim 5.7 \times 4.5$  in. and height of 6.5 in. Note that the printed magnet was coated by TruDesign, LLC using a clear polyurethane polymer. The inner wall of the cylinder shows the layer-upon-layer structure of the printed magnet.

Table 2 shows a comparison of the characteristics of BAAM and the conventionally injection molded (IM) magnets made from the same starting materials (65 vol.% MQP B+ and 35 vol.% Nylon-12) by Magnet Application Inc. Note that the primary magnetic characteristics of permanent magnets are intrinsic coercivity  $H_{ci}$  (the ability to resist demagnetization), remanence  $B_r$  (residue magnetization upon the removal of magnetic field), and energy product  $BH_{max}$  (the maximum magnetostatic energy a magnet can store). It was mentioned that the density of the printed part is essential as it determines the magnetic flux the magnet can generate in a given space, assuming the same starting materials and that the magnetic properties are not degraded during the fabrication process. In some sense, printing stronger bonded magnets means increasing the packing density of the magnetic particles. Here, the measured densities of BAAM and IM magnets are very close, namely  $\sim 4.9$  g/cm<sup>3</sup>. However, this value is 8% lower than the theoretical limit of 5.3 g/cm<sup>3</sup> which can be calculated from the starting nominal composition of 65 vol.% loading fraction of magnetic particles in a polymer. For comparison, the densities of 3D printed magnet and IM magnet reported by Huber *et al.* are 3.6 g/cm<sup>3</sup> and 4.4 g/cm<sup>3</sup>, which are 22% and 4% lower than the theoretical limit of 4.6 g/cm<sup>3</sup> calculated from the starting nominal composition of 54 vol.% loading fraction, respectively, indicating a higher level of porosity in 3D printed magnets. Both BAAM and IM magnets show a slight deterioration in  $H_{ci}$  as compared to the starting pellets which have a  $H_{ci} = 8.9$  kOe. These deteriorations can be attributed to the grain growth/microstructure change caused by the heating during the melting process. It is possible that the IM machine may have gone through a slightly higher temperature and/or residence time during printing compared to the BAAM extruder. Consequently, the IM magnets may have a lower coercivity as compared to BAAM magnets. The small variation in  $B_r$  between BAAM and IM magnets possibly results from the different geometries of the magnetization sample, as the magnetization was measured with an “open loop” vibrating sample magnetometer, and the demagnetization correction was not performed. On the other hand, the rapid cooling feature of 3D printing creates internal residual stress, possibly causing mechanical property degradations and structure deformations. Note that the ultimate tensile strength (UTS) and ultimate strain for IM magnets in Table 2 are taken from Ref. [26] for magnets made from 60 vol.% melt-spun irregular

shaped powders. The UTS of the 3D printed magnets is significantly direction dependent, with the z direction (part growth direction) being the weakest. This directional dependence is typical for all layered additive manufacturing techniques. The z-direction strength typically represents process dependent interface properties between layers, rather than the properties of the underlying material. Here, the tensile testing on the BAAM magnets was done along x axis which is perpendicular to the printing direction [25]. It can be seen from Table 2 that the IM magnets exhibit higher UTS but lower ductility. It was suggested that the separation of the magnetic particles from the nylon binder is the primary failure mechanism during the tensile test for bonded magnets [25, 26]. SEM images of the BAAM magnets [25] revealed some voids, primarily located at the interface between the magnetic particle and the binder, which could account for the lower UTS. One well-known drawback of NdFeB magnets is the rapid reduction in intrinsic coercivity  $H_{ci}$  and energy product  $BH_{max}$  with rising temperature, limiting its high temperature operation. The temperature coefficient of  $BH_{max}$  is  $-0.26$  and  $-0.32\%/^{\circ}\text{C}$  for BAAM and IM magnets, which indicate that when the temperature is increased from 25 to 125  $^{\circ}\text{C}$ , the BAAM and IM magnets will experience a  $BH_{max}$  loss of 26% and 32%, respectively. Thus the BAAM magnet has a slightly better thermal stability. In fact, coating with a polymer protective layer is usually required to improve thermal stability and corrosion resistance, which is outside the scope of this viewpoint.

The magnetic powder volume fraction ( $f$ ) is very important for bonded magnets as the energy product is proportional to  $f^2$ . It was shown that the UTS also increases with  $f$  [26]. Volume fraction of magnetic powder in commercial injection molded and compression bonded magnets is typically 65% and 80%, respectively. Our next effort is to increase  $f$  to beyond 65 vol.% for BAAM 3D printing, with an ultimate goal of achieving the same energy product  $BH_{max}$  as that of the compression molded magnets. In addition, BAAM printing with anisotropic powder is also underway.

## 5. Outlook

AM has been commercially used in various areas, including aerospace, automotive, energy, and lightweight, highly efficient structures

**Table 2**

Characteristics of the BAAM magnet vs. IM magnet. Note that the magnetic properties and mechanical properties of the BAAM magnets are taken from Ref. [25], and the mechanical properties of the IM magnets are taken from Ref. [26].

Method	Density (g/cm <sup>3</sup> )	$H_{ci}$ (kOe)	$H_c$ (kOe)	$B_r$ (kG)	$BH_{max}$ (MGOe)	Temperature coefficient of $BH_{max}$ [%/ $^{\circ}\text{C}$ ]	UTS (MPa)	Ultimate strain [%]
BAAM	4.9	8.7	4.1	5.0	5.3	$-0.26$	6.6	4.2
IM	4.8	8.0	3.6	4.8	4.6	$-0.32$	18.4	0.4

for the transportation sector. A detailed evaluation of the competitiveness of AM for producing parts with varying geometric complexity, customization, and production volume is given in Ref. [27]. In general, AM is suited for low to medium volume production especially when customized design is desired. Nevertheless, AM suffers from accuracy issues due to the distortion and residual stress buildup during the layering process [28]. A direct link between the property of the feedstock material, extrusion nozzle diameters, printing parameters, and the mechanical and functional properties of the resulting parts needs to be built to ensure repeatability. Significant advancements are necessary for AM to replace the conventional techniques for fabricating high volume parts with a relatively simple shape. Nevertheless, to the least extent, AM can be employed as a tool in the design and development of innovative motor magnets, whereby a better motor design that enables fullest use of the magnetic flux would in turn save RE consumption. What's more, the motor which consists of non-magnetic frames (e.g., stator, rotator, etc.) and permanent magnets, can be printed as a single part, enabling higher accuracy and shorter design-to-part time. BAAM is more prominent compared to binder jetting in terms of producing mechanically and magnetically useful parts. Injection molding is the commercial method that BAAM can outperform, with an ultimate goal of rivaling compression molding.

Fig. 3 shows a spiderweb chart comparing different characteristics (i.e.,  $BH_{max}$ , UTS, ultimate strain, reduced critical material waste, and reduced weight  $\times$  cost) for sintered, injection molded (IM), and additively printed (AM) bonded magnets. IM and AM have similar capabilities, with AM showing a slight advantage in terms of reducing material waste and reducing weight  $\times$  cost, and mechanically, lower UTS and superior ductility. Sintered magnets have much higher energy product, higher tensile strength, and on the other hand, much higher critical RE waste and therefore higher weight  $\times$  cost. Note that the estimated weight  $\times$  cost for sintered and injection molded magnets is resourced from Aichi Steel Inc. Currently, permanent magnet synchronous motors generally employ sintered NdFeB magnets owing to their highest residual flux density. However, the high electrical conductivity of sintered magnets results in severe eddy current loss, which reduces the motor efficiency [29]. It was demonstrated by both simulation and experimental results that the axial gap motor employing NdFeB bonded magnets can attain both higher torque and higher efficiency compared with the radial gap motor incorporating NdFeB sintered magnets with the same weight of magnets [30]. This inspiring work further validates the motivation to develop advanced manufacturing technologies like 3D printing to fabricate bonded magnets. It is important to note that the 3D printing methods discussed in this viewpoint are not exclusive to NdFeB-based magnets, but can be applied to the fabrication of a wide range of magnetic materials and compositions.

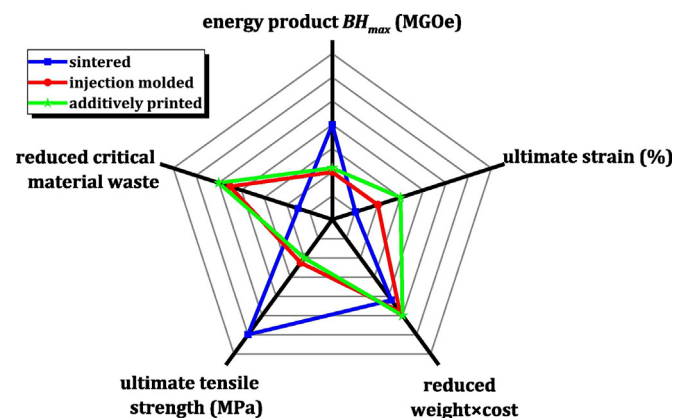


Fig. 3. A spider chart comparing different characteristics between sintered, injection molded, and additively printed magnets.

In summary, AM offers an economical method to fabricate RE-based bonded magnets with no limitations in geometry and quantities. However, the following challenges remain to be addressed to facilitate industrial applications:

- 1) A detailed microstructural and/or residual stress study is needed to optimize the printing parameter.
- 2) Optimization of the extrusion nozzle diameters, extrusion temperatures and residence time and starting magnet particle size are also necessary.
- 3) A mature system for *in-situ* magnetic field alignment of the anisotropic powder during the printing process needs to be designed and implemented.
- 4) Techno-economic analysis of the AM in order to compete with traditional IM techniques.

## 6. Concluding remarks

Demand for magnets is expected to experience a substantial increase with the maturation of clean energy technologies, which has already opposed a concern regarding the supply of RE elements. With the significant advantage of minimum material waste and no tooling requirement, AM offers an economical method to fabricate near-net-shape magnets with no quantity restrictions. The shape flexibility of AM magnets unleashes opportunities for motor designers, and is also beneficial in sensor technology. Nevertheless, AM printing of magnets is still in its infancy. While we demonstrate that material extrusion is capable of fabricating bonded magnets with magnetic and mechanical properties comparable to those of conventionally injection molded magnets, extensive research needs to be done to acquire a thorough understanding of the correlation between the property of the feedstock materials, printing parameters, and the mechanical and magnetic properties of the resulting bonded magnets, to ensure repeatability and consistency in the printed parts.

## Acknowledgment

This work was supported by the Critical Materials Institute, an Energy Innovation Hub funded by the U.S. Department of Energy, Office of Energy Efficiency and Renewable Energy, Advanced Manufacturing Office. Access to the MDF facilities and use of additive instrument time and labor are supported by the MDF Tech Collaborations between ORNL and Magnet Applications Inc./Tru Design LLC. Thanks are due to John Ormerod and Robert Fredette from Magnet Applications for supplying nylon magnet composite pellets for 3D printing. Thanks are also due to Rick Spears from Tru Design for help with finishing the 3D printed parts.

Notice: This manuscript has been authored by UT-Battelle, LLC under Contract No. DE-AC05-00OR22725 with the U.S. Department of Energy. The United States Government retains and the publisher, by accepting the article for publication, acknowledges that the United States Government retains a non-exclusive, paid-up, irrevocable, world-wide license to publish or reproduce the published form of this manuscript, or allow others to do so, for United States Government purposes. The Department of Energy will provide public access to these results of federally sponsored research in accordance with the DOE Public Access Plan (<http://energy.gov/downloads/doe-public-access-plan>).

## References

- [1] J.M.D. Coey, J. Magn. Magn. Mater. 248 (3) (2002) 441–456.
- [2] J.M.D. Coey, Scr. Mater. 67 (6) (2012) 524–529.
- [3] A.K. Pathak, K.A. Gschneidner, M. Khan, R.W. McCallum, V.K. Pecharsky, J. Alloys Compd. 668 (2016) 80–86.
- [4] B.C. Sales, B. Saparov, M.A. McGuire, D.J. Singh, D.S. Parker, Sci. Rep. 4 (2014) 7024.
- [5] H.L. Tekinalp, V. Kunc, G.M. Velez-Garcia, C.E. Duty, L.J. Love, A.K. Naskar, C.A. Blue, S. Ozcan, Compos. Sci. Technol. 105 (2014) 144–150.

- [6] L.E. Murr, S.M. Gaytan, D.A. Ramirez, E. Martinez, J. Hernandez, K.N. Amato, P.W. Shindo, F.R. Medina, R.B. Wicker, *J. Mater. Sci. Technol.* 28 (1) (2012) 1–14.
- [7] W.E. Frazier, *J. Mater. Eng. Perform.* 23 (6) (2014) 1917–1928.
- [8] B. Baufeld, O.V.d. Biest, R. Gault, *Mater. Des.* 31 (2010) S106–S111.
- [9] J. Geng, I.C. Nlebedim, M.F. Besser, E. Simsek, R.T. Ott, *JOM* 68 (7) (2016) 1972–1977.
- [10] C. Huber, C. Abert, F. Bruckner, M. Groenefeld, O. Muthsam, S. Schuschnigg, K. Sirak, R. Thanhoffer, I. Teliban, C. Vogler, R. Windl, D. Suess, *Appl. Phys. Lett.* 109 (16) (2016) 162401.
- [11] B.G. Compton, J.W. Kemp, T.V. Novikov, R.C. Pack, C.I. Nlebedim, C.E. Duty, O. Rios, M.P. Paranthaman, *Mater. Manuf. Process.* (2016).
- [12] Y. Huang, M.C. Leu, J. Mazumder, A. Donmez, *J. Manuf. Sci. Eng.* 137 (1) (2014) 014001.
- [13] J. Ormerod, S. Constantinides, *J. Appl. Phys.* 81 (8) (1997) 4816.
- [14] D.N. Brown, *IEEE Trans. Magn.* 52 (7) (2016) 1–9.
- [15] M.P. Paranthaman, C.S. Shafer, A.M. Elliott, D.H. Siddel, M.A. McGuire, R.M. Springfield, J. Martin, R. Fredette, J. Ormerod, *JOM* 68 (7) (2016) 1978–1982.
- [16] G. Manogharan, M. Kioko, C. Linkous, *JOM* 67 (3) (2015) 660–667.
- [17] Y. Bai, C.B. Williams, *Rapid Prototyp. J.* 21 (2) (2015) 177–185.
- [18] S.M. Gaytan, M.A. Cadena, H. Karim, D. Delfin, Y. Lin, D. Espalin, E. MacDonald, R.B. Wicker, *Ceram. Int.* 41 (5) (2015) 6610–6619.
- [19] H. Miyajima, S. Zhang, A. Lassell, A. Zandinejad, L. Yang, *JOM* 68 (3) (2016) 831–841.
- [20] A. Elliott, S. AlSalhi, A.L. Merriman, M.M. Basti, *Am. J. Eng. Appl. Sci.* 9 (1) (2016) 128–133.
- [21] H. Sepehri-Amin, T. Ohkubo, T. Nishiuchi, S. Hirose, K. Hono, *Scr. Mater.* 63 (11) (2010) 1124–1127.
- [22] T. Akiya, J. Liu, H. Sepehri-Amin, T. Ohkubo, K. Hioki, A. Hattori, K. Hono, *Scr. Mater.* 81 (2014) 48–51.
- [23] I.C. Nlebedim, H. Ucar, C.B. Hatter, R.W. McCallum, S.K. McCall, M.J. Kramer, M.P. Paranthaman, *J. Magn. Magn. Mater.* 422 (2017) 168–173.
- [24] C. Holshouser, C. Newell, S. Palas, L.J. Love, V. Kunc, R. Lind, P.D. Lloyd, J. Rowe, R.R. Dehoff, W. Peter, C. Blue, *Adv. Mater. Process.* 171 (2013) 15–17.
- [25] L. Li, A. Tirado, I.C. Nlebedim, O. Rios, B. Post, V. Kunc, R.R. Lowden, E. Lara-Curzio, R. Fredette, J. Ormerod, T.A. Lograsso, M.P. Paranthaman, *Sci. Rep.* 6 (2016) 36212.
- [26] M.G. Garrell, A.J. Shih, B.-M. Ma, E. Lara-Curzio, R.O. Scattergood, *J. Magn. Magn. Mater.* 257 (1) (2003) 32–43.
- [27] B.P. Conner, G.P. Manogharan, A.N. Martof, L.M. Rodomsky, C.M. Rodomsky, D.C. Jordan, J.W. Limperos, *Addit. Manuf.* 1–4 (2014) 64–76.
- [28] M.R. Talagani, S. DorMohammadi, R. Dutton, C. Godines, H. Baid, F. Abdi, V. Kunc, B. Compton, S. Simunovic, C. Duty, L. Love, B. Post, C. Blue, *SAMPE J.* 51 (4) (2015) 27–36.
- [29] K. Yamazaki, M. Shina, M. Miwa, J. Hagiwara, *IEEE Trans. Magn.* 44 (11) (2008) 4269–4272.
- [30] R. Tsunata, M. Takemoto, S. Ogasawara, A. Watanabe, T. Ueno, K. Yamada, 2016 XXII International Conference on Electrical Machines (ICEM) 2016, pp. 272–278.